BLAST-INDUCED FRACTURING AROUND BOREHOLES AND GAS-PRESSURISED RAPID CRACK EXTENSION

A. DAEHNKE*, N. KOUZNIAK**, H.P. ROSSMANITH** and R.E. KNASMILLNER**
*CSIR Mining Technology, Auckland Park 2006, Johannesburg, South Africa
**Vienna University of Technology, Wiedner Hauptstr. 8-10/325, A-1040 Vienna, Austria

ABSTRACT

To give insights into mechanisms creating damage and fracture zones in the immediate borehole vicinity, as well as gas pressurisation mechanisms, three-dimensional cube-type laboratory models fabricated from PMMA are dynamically loaded with explosives and the resulting contained fracture network is studied. A coupled solid, fluid and fracture mechanics numerical model is used to analyse the gas driven fracture propagation phase of blast-induced fracturing. The model incorporates dynamic material properties and quasi-dynamic fracture mechanics, can predict propagation rates and provides pressure profiles and gas velocities within the fractures. The numerically calculated fracture speed and fracture extent are compared with data observed in the experiments.

KEYWORDS

Dynamic fracture propagation, blast-induced fracturing, gas-driven fracturing, PMMA.

INTRODUCTION

The study deals with the formation of blast-induced damage and fracture zones, and the propagation of cracks from the borehole. Kutter and Fairhurst (1971) were among the first to consider the complex coupling of solid, fracture and fluid mechanics in blast-induced fracturing, and they divided the blast problem into two phases:

(i) Stress wave dominated phase: the stress waves emerging from the blast hole initiate local damage and fracturing around the borehole.

(ii) Gas pressure dominated phase: the penetration of the rapidly expanding gaseous combustion products causes the extension of long radial cracks.

Subsequent investigators adopted this two-phase approach, as was the case in this work. Laboratory experiments were conducted to investigate the fracture network due to blast-induced cracking both in the near and far field.

EXPERIMENTAL PROCEDURE

Controlled three-dimensional laboratory experiments in transparent PMMA cubes (250 x 250 x 240 mm^3) were conducted and, by means of high speed photographic techniques, the evolution of blast induced fractures was recorded. A Cranz-Schardin (C-S) multiple spark gap camera provides 24 'snap-shot' frames of the dynamic process photographed at discrete time intervals at a framing rate of 50 000 to 280 000 frames per second. The use of circularly polarised monochromatic light, in conjunction with the bi-refringent material property of PMMA, permits the recording of isochromatic fringe patterns of the propagating stress waves (an isochromatic contour is a line of equal maximum shear stress). Thus the exact fracture front and stress wave position in time can be recorded for further assessment of fracture growth.

In laboratory experiments Kutter and Fairhurst (1971) found that blast induced fracture patterns in laboratory models fabricated from PMMA are similar to those in equivalent models constructed from homogeneous monolithic blocks of rock. As the objective of this investigation was to understand the underlying mechanisms governing dynamic fracture, PMMA was chosen as a suitable material to study fracture mechanisms which also apply to brittle rock. The results of two series of laboratory experiments are discussed below:

(i) An unstemmed column charge was detonated in a PMMA cube to study the near-borehole damage and fracture zone.
(ii) By detonating a short cylindrical sealed charge in a PMMA cube the mechanism of fracture extension by gas pressurisation was investigated.

STRESS WAVE DOMINATED PHASE

Upon detonation, the immediate vicinity of the borehole is highly strained and the local conditions in the borehole, e.g. the degree of coupling between column charge and borehole wall, pre-existing flaws in the borehole wall etc., will influence the borehole fragmentation. Over many decades, numerous experimental and theoretical studies of blasting in different materials were conducted. Generally authors distinguish between three annular zones surrounding the borehole: the innermost zone, a transitional zone with short dense cracks, and an outer elastic zone with long radial cracks. In the case of shock wave propagation in metals, Davis and Calvit (1963) identify an innermost zone around the hole in which the material behaves in a fluid-like manner with no cracks whatsoever visible. Similar results were obtained by Persson *et al.* (1970) when blasting laboratory scaled models fabricated from PMMA cubes. The blasting behaviour of glass and rock materials, studied in several papers by Kutter and Fairhurst (1971), Rossmanith (1978), Fourney *et al.* (1983), Singh and Sarma (1983), Swoboda and Li (1993), Liu and Katsabanis (1993) and others, revealed a highly crushed zone around the borehole instead of a fluidised regime characterised by the complete absence of cracks and damage.

Experimental Program and Results

Numerous experiments were conducted to investigate the processes in the near-borehole zone. For the experiment described here a column charge is detonated in a PMMA cube. The column charge (66 mm long and 3 mm diameter) consists of 620 mg tightly packed PETN which was left unstemmed, thus allowing the combustion gases to vent. Figure 1 a) shows the final fracture network in a plane normal to the borehole axis, and Fig. 1 b) gives an enlarged view of the borehole vicinity. It is seen here that a system of short radial cracks has propagated from

the borehole wall. The length of these cracks is approximately 3 times the initial radius of the borehole. This innermost zone is marked in Figs 1 a) and b) by 'A'. In addition, a few circumferential cracks initiated inside Zone A can be identified in the lower part of Fig. 1 b). A longitudinal cross-section of the cube along the borehole axis revealed that these circumferential cracks extend parallel to the borehole along most of its length. It is thought that these were formed due to the tensile trailing tail of the radial stress pulse, which is known to achieve its maximum value at some distance from the hole (Kutter and Fairhurst, 1971). Termination of the circumferential cracks at the radial cracks led to the formation of pie-shaped segments, 'p', which are dislocated towards the borehole. In certain cases the combined effect of radial and circumferential cracks might lead to severe borehole damage. After detonation of the explosive the borehole was vacuum impregnated with dyed Araldite D. It was found that the dye was contained within Zone A, indicating that only within this zone did the cracks remain open.

It is observed that most of the radial cracks extending from Zone A into Zone B become kinked (or branched). Only a few new cracks born in Zone B have been identified. Most cracks in Zone B propagate at some angle to the radial direction. Zone B is often referred to in literature as a 'shear crack zone' (Persson *et al.*, 1970).

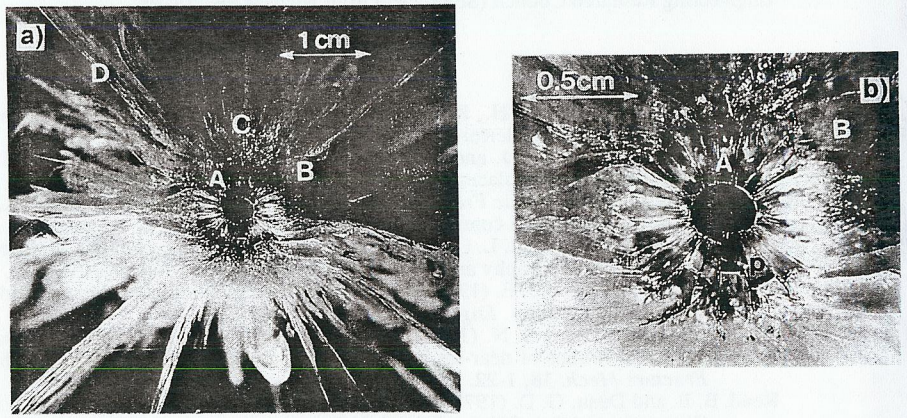

Fig. 1: Fracture network in a plane normal to borehole.

The third relatively small zone labelled 'C' is formed by subsequent kinking of numerous cracks emerging from Zone B, and most of these fractures reorient themselves in a radial direction. Finally, only some of the cracks in Zone D propagate towards the free surfaces of the cube, with few of them surfacing. It is believed that the main driving mechanism of the cracks in Zone D is the pressurisation by combustion gases. The results of this new series of experiments prove that damage processes in the borehole vicinity are still not well understood and small deviations in blasting conditions, configurations or material parameters may lead to fracture networks quite different to those described previously in literature. For example, contrary to the densely cracked Zone A observed in this work, Persson *et al.* (1970) reported a non-cracked innermost zone in a similar experiment using the same charge type and borehole diameter in a PMMA block. Further investigations are required.

Borehole Pressure

A theoretical study was conducted to gain insights into the borehole pressure magnitudes. The approach uses known fracture mechanics formulas to calculate borehole pressures required for fracture initiation from borehole wall flaws. As the explosive detonates, the resulting pressure of the combustion gas acts on the borehole walls and microflaws around the borehole, which are either inherent material inhomogeneities or man-made imperfections caused by drilling, are activated and grow to form fractures. The fractures are driven by two mechanisms, (i) the stress distribution around the pressurised borehole with no gas pressure acting on the crack faces, (ii) the fractures themselves are pressurised by detonation gases and are thus extended. Initially the borehole stress is the dominating crack driving mechanism, however as the fractures extend the gas entering the fractures becomes the main driving force. Generalised integral formulas (Nilson and Proffer, 1984) based on the weight function technique are used to calculate the stress intensity factor for wedge- and disk-shaped cracks propagating from cylindrical boreholes.

The above approach was used in a static analysis to estimate the minimum borehole pressure required to drive fractures for the experiment described previously. The borehole pressure was calculated such that the stress intensity factor for flaws ranging from 1 μm to 1.5 mm was equal to the fracture toughness of PMMA. The required pressure for fracture initiation was calculated taking into account static (1.0 MN $m^{-3/2}$) and dynamic (4.5 MN $m^{-3/2}$) fracture toughness according to values measured experimentally by Green and Pratt (1974) for PMMA up to a fracture velocity of c = 500 m/s. This is considered to represent the upper bound of the fracture velocity during initial borehole cracking (Hernandez Gomez and Ruiz, 1993). Figure 2 gives a chart relating borehole pressure to flaw size for a wedge-shaped fracture propagating from a cylindrical borehole.

It is evident from Fig. 2 that required pressures are unlikely to exceed 360 MPa for flaw sizes of approximately 10 μm and 122 MPa for flaw sizes of 100 μm. This range in flaw sizes is considered to be realistic for a borehole drilled into PMMA. Using the static fracture toughness of PMMA, the required borehole pressure for fracture initiation from flaws ranging in size from 1 μm to 1.5 mm was calculated for wedge-shaped and disk-shaped fractures. As indicated in Fig. 3, disk-shaped fractures require a higher pressure for fracture initiation from a given flaw size.

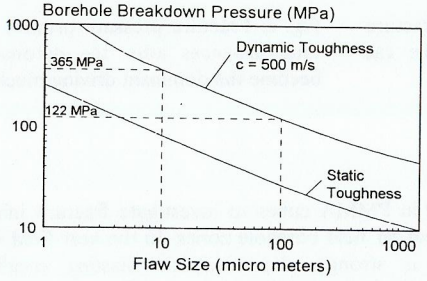

Fig. 2: Minimum required borehole breakdown pressure for a wedge-shaped fracture.

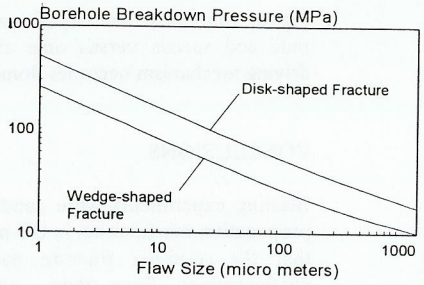

Fig. 3: Borehole breakdown pressure for wedge- and disk-shaped fractures.

This is in agreement with the fracture orientation observed in the experiment, were the fractures are exclusively radial in orientation and no disk-shaped fractures are formed. The only exception is a cone-shaped fracture which has propagated from the perimeter of the borehole end.

GAS DRIVEN FRACTURE PROPAGATION

Previous work (Fourney *et al.*, 1979; Worsey *et al.*, 1981 and McHugh, 1983) concluded that in many cases the second stage, i.e. gas driven fracture propagation, is the dominant mechanism in extending long fractures, and it is feasible that the gas pressurisation increases the fracture length by a factor of 10-100 as compared with crack extension due to the stress wave loading alone (McHugh, 1983).

A numerical procedure proposed by Nilson (1986) is used to analyse crack propagation due to high pressure combustion gases. The method is used to model gas flow within penny-shaped fractures, where the gas is fed from a centrally located borehole. Frictional losses as well as convective and conductive heat transfer from the hot combustion gases to the fracture walls are taken into account. Here Nilson's approach is extended to incorporate dynamic material properties and quasi-dynamic fracture mechanics. Results of laboratory experiments conducted with three-dimensional cube type specimens are given, and numerically calculated and experimentally observed fracture propagation rates and fracture lengths are correlated.

Numerical Analysis

A combined analytical/numerical integral method is used to model the flow of high pressure combustion products into a propagating penny-shaped fracture. Mathematical models of explosively driven fracturing incorporate several disciplines such as fluid mechanics, elasticity, fracture mechanics and heat transfer. These aspects are closely coupled as the opening displacement depends on the pressure distribution, which is controlled by fluid friction, which in turn depends upon the fracture aperture. Such severe coupling usually precludes an exact analytical solution of the governing equations. In the method used here the pressure distribution along the fracture is described by a four-parameter family of curves. At each time step the parameters are numerically determined such that the stress intensity factor attains the critical value and the conservation equations are satisfied. The fluid flow along the fracture is governed by the laws of mass, momentum and energy conservation, and for one-dimensional fluid transport the governing equations are given by Shapiro (1954), Nilson *et al.* (1985). Fluid drag is incorporated through the friction factor based on experimental data (Huitt, 1956) for turbulent flow in geologic fractures.

Using high-speed photography Green and Pratt (1974) measured the dynamic fracture toughness of PMMA, and found the dynamic fracture toughness to approximately linearly depend on the crack speed, and this dependence is incorporated in the numerical analysis. Inertial effects of rapidly propagating fractures are accounted for by including a dynamic stress intensity factor as proposed by Freund (1972), who found that the dynamic stress intensity factor varies almost linearly with the crack speed, from the static value at zero speed to zero at the Rayleigh wave speed.

The input to the numerical analysis consists of the detonation temperature and detonation pressure. The detonation temperature can be obtained from the Rankine-Hugoniot equations

(Persson *et al.*, 1994). For Lead Azide, at the density used in the experiments, it is approximately 2700 K. Borehole pressurisation is assumed to occur instantaneously, as the detonation wave propagates through the explosive in less than 1 μs. Thus, relative to the total time period of fracture extension, the effect of the borehole pressure rise as the explosive detonates is negligible. The initial borehole pressure is taken to be 160 MPa. This pressure level is chosen to yield an initial fracture propagation rate and overall fracture extension of similar magnitude as observed in the experiments. During the initial phase the fractures are assumed to be driven by stress waves, and as these outpace the fractures, combustion gas induced cracking takes over as the propagating mechanism. In the calculation the cracks are assumed to have extended 12 mm due to stress wave loading, and only the subsequent crack extension due to gas pressurisation is modelled numerically.

Experimental Program

A laboratory model with a totally sealed charge was constructed by bonding two PMMA slabs together with the explosive encased in the centre. The explosive was triggered and ignited by thin copper wires bonded between the slabs which conduct the 2 kV triggering pulse. The slabs were glued together with liquid PMMA, resulting in a homogeneous PMMA cube. A micro-charge (160 mg Lead Azide, 5 mm diameter and 5 mm length) of explosive was appropriately tailored to (i) prevent the fractures from surfacing at the cube sides and venting their gas content, and (ii) minimise the interaction effect between reflected stress waves and the gas-driven fractures.

Two dish-shaped conical fractures (Fractures A and B in Fig. 4) have propagated from the circular ends of the cylindrical charge cavity which act as discontinuities. These dish-shaped fractures represent most of the fracture area, and the fractures parallel to the borehole axis linking the two main dish-shaped fractures (e.g. Fracture C) are much smaller.

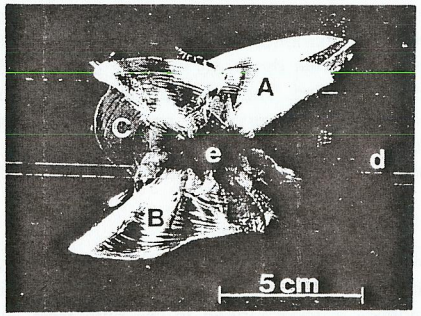

Fig. 4: Final fracture structure of sealed charge experiment. Here *e* refers to the position of the explosive charge and *d* to the detonation wire.

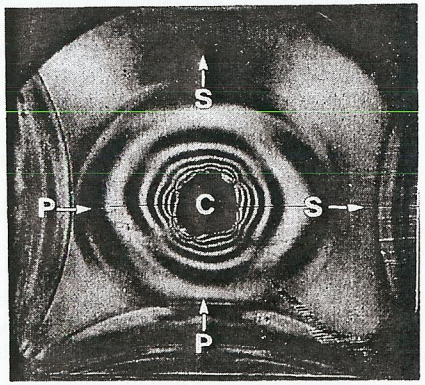

Fig. 5: Photograph showing fracture (Label C) and stress wave positions 65 μs after charge detonation.

Figure 5 highlights an instant in time 65 μs after charge detonation of the dynamic fracture propagation and stress waves for the sealed charge experiment. Isochromatic contours corresponding to the position of the reflected longitudinal wave, which has been reflected by the cube boundaries and is now propagating at c_P = 2500 m/s back towards the model centre, are visible (Label P), whilst the isochromatic contours associated with the outgoing shear waves propagating at c_S = 1400 m/s are labelled by S. As shown in Fig. 5, the longitudinal stress wave rapidly out-paces the fractures propagating at a much slower rate, and hence fractures extend mainly due to pressurisation by combustion gases.

Correlating Experimental and Numerical Results

The conical fractures observed in the laboratory experiments (Fractures A and B in Fig. 4) can be approximated as two penny-shaped fractures propagating from a centrally located pressurised borehole. The evolution of these fractures was used for fine-tuning the input parameters for the numerical procedure. Figure 6 shows experimental data and calculated fracture radius and speed versus time pertaining to the phase where the detonation gases have become the fracture driving mechanism. Figure 7 shows the calculated pressure profiles in the propagating fracture at various time instances.

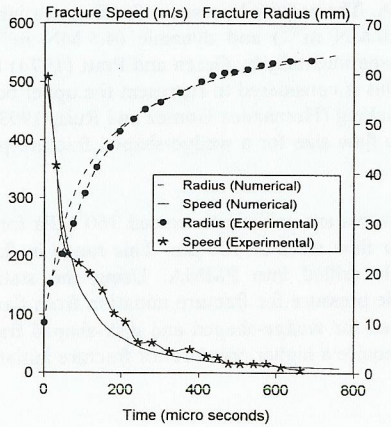

Fig. 6: Numerical and experimental fracture radii and speeds versus time after the gas driving mechanism becomes dominant.

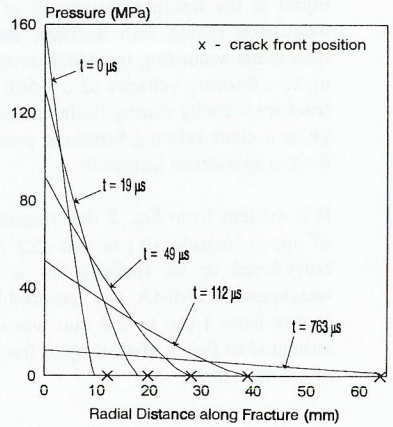

Fig. 7: Fracture pressure profiles at various time instances after the detonation gases become the dominant driving mechanism.

CONCLUSIONS

Blasting experiments were conducted in PMMA cubes to investigate fracture initiation and propagation mechanisms in the near and far field borehole zones. In the near field it is shown that the resulting fracture pattern is strongly dependant on blasting conditions and configurations. Four zones are identified and qualitatively described, and discrepancies between these and fracture networks described in literature are outlined. A coupled solid, fluid and fracture mechanics numerical model is used to analyse the gas driven fracture propagation phase. Fracture propagation velocity and the final fracture extent calculated by the numerical

model are compared with results from a laboratory experiment, and good correlations between numerical and experimental findings are observed.

REFERENCES

Davis, N. and H.H. Calvit (1963). Some dynamical applications of shock wave propagations in solids. In: *Stress Waves in Anelastic Solids, IUTAM Symposium*, pp. 1-19.

Fourney, W.L., D.C. Holloway and D.B. Barker (1979). Fracture initiation from the packer area. *University of Maryland Research Report prepared for the National Science Foundation.*

Fourney, W.L., D.B. Barker and D.C. Holloway (1983). Fragmentation in jointed rock material. In: *Rock Fragmentation by Blasting. Proc. 1st Int. Symp.*, pp. 505-531, Lulea University of Technology, Sweden.

Freund, L.B. (1972). Crack propagation in an elastic solid subjected to general loading - I. Constant rate of extension. *J. Mech. Phys. Solids,* 20, 129-140.

Green, A.K. and P.L. Pratt (1974). Measurement of the dynamic fracture toughness of Polymethylacrylate by high-speed photography. *Eng. Fract. Mech.,* 6, 71-80.

Hernandez Gomez, L.H. and C. Ruiz (1993). Experimental evaluation of crack propagation velocity in PMMA under dynamic pressure loading. *Int. J. of Fracture,* 61, 21-28.

Huitt, J.L. (1956). Fluid flow in simulated hydraulic fractures. *AIChE J.,* 2, 2, 259-264.

Kutter, H.K. and C. Fairhurst (1971). On the fracture process in blasting. *Int. J. Rock Mech. Min. Sci.,* 8, 181-202.

Liu, G. and P.D. Katsabanis (1993). A theoretical approach to stress waves around a borehole and their effect on rock crushing. In: *Rock Fragmentation by Blasting,. 4th Int. Symp.*, pp. 9-16, Balkema, Rotterdam.

McHugh, S. (1983). Crack extension caused by internal gas pressure compared with extension caused by tensile stress. *Int. J. of Fracture,* 21, 163-176.

Nilson, R.H. and W.J. Proffer (1984). Engineering formulas for fractures emanating from cylindrical and spherical holes. *J. Appl. Mech.*, 51, 929-933.

Nilson, R.H., W.J. Proffer and R.E. Duff (1985). Modelling of gas-driven fractures induced by propellant combustion within a borehole. *Int. J. Rock Mech. Min. Sci. & Geomech. Abstr.*, 22, 1, 3-19.

Nilson, R.H. (1986). An integral method for predicting hydraulic fracture propagation driven by gases or liquids. *Int. J. for Num. and Analyt. Methods in Geomech.,* 10, 191-211.

Persson, P.A., N. Lundborg and C.H. Johansson (1970). The basic mechanisms in rock blasting. In: *Proc. 2nd Congr. Int. Soc. Rock Mech.*, pp. 1-15.

Persson, P., R. Holmberg and J. Lee (1994). In: *Rock Blasting and Explosives Engineering*. CRC Press.

Rossmanith, H.P. (1978). Dynamic fracture in glass. *University of Maryland Research Report prepared for the National Science Foundation.*

Shapiro, A.H. (1954). In: *The Dynamics and Thermodynamics of Compressible Fluid Flow*. Ronald Press, New York.

Singh, D.P. and K.S. Sarma (1983). The influence of joints on rock blasting. In: *Rock Fragmentation by Blasting. Proc. 1st Int. Symp.,* pp. 533-554, Lulea University of Technology, Sweden.

Swoboda, G. and N. Li (1993). Numerical modelling of blast loading. In: *Rock Fragmentation by Blasting. Proc. 4th Int. Symp.,* pp. 25-31, Balkema, Rotterdam.

Worsey, P.N., I.W. Farmer and G.D. Matheson (1981). The mechanics of pre-splitting in discontinuous rock. In: *Proc. 22nd U. S. Symposium on Rock Mechanics,* pp. 218-223, Massachusetts Institute of Technology.